Indian Geotechnical Journal, 41(4), 2011, 186-195

Liquefaction and Post Liquefaction Behaviour of Granular Materials: Particle Shape Effect

Anitha Kumari S. D.[1] and T. G. Sitharam[2]

Key words

DEM, particle shape, liquefaction, post liquefaction

Abstract: The discrete nature of the granular mass plays a very significant role in the liquefaction and post liquefaction behaviour. Liquefaction occurs when a granular mass completely loses its shear strength. The stress-strain response of the liquefied mass is significant in understanding the granular assembly's resistance to the monotonically increasing static loads following liquefaction. Majority of the research on liquefaction and post-liquefaction behaviour from a grain scale have been done considering the particle shape as spherical. But it is proven that the particle shape has significant effect on the mechanical behaviour of a given soil mass. Hence in this study, the particles with different shapes are modeled and their behavior under cyclic loading is studied. Once these samples liquefy, they are subjected to monotonic undrained shear testing to understand the post liquefaction behavior. An assembly similar to a triaxial specimen is modeled and subjected to cyclic loading. The effects of parameters like confining pressure and the number of cycles of load application on the behaviour of the granular mass with particles of arbitrary shapes are presented. The studies clearly indicate that as the particle shape changes, there is an increase in the strength due to interlocking. Also, the number of cycles required for liquefaction is more for shapes other than spheres. These factors are explained on the basis of the micromechanical aspects like average coordination number, contact force, contact distribution etc.

Introduction

Generally the modeling of soil behaviour is done at the macro-scale without giving much emphasis on the microscale behaviour. The state of knowledge related to liquefaction and its associated phenomena has been studied in detail during the last few decades by analytical and laboratory experiments (Seed & Lee, 1966, Ishihara et al., 1975). But limited number of studies has been done to understand this phenomenon from a grain level which can shed light into the fundamental aspects of cyclic behaviour. The discrete character of the medium results in microscale interaction between particles. The magnitude and direction of the contact forces greatly depends upon the initial state of the sample and the anisotropic state of the assembly. As the loading progresses, the grains deform, contacts are made and lost and contact forces are changed.

Numerical simulations using Discrete Element Method (DEM) (Cundall and Strack ,1979) can provide information on stresses, strains, average coordination number, contact forces, contact normal etc. during any stage of loading. Studies have been done on liquefaction behaviour using DEM by Ng and Dobry (1994), Sitharam et al (2002), Sitharam (2003), Sitharam and Vinod (2008) considering spherical particles. Norris et al. (1997) predicted the undrained response from drained triaxial tests and indicated that the constant volume simulations and the undrained tests on saturated sands with pore pressure measurements give similar results. Hence numerical simulations of undrained tests are done by adopting the constant volume approach. Sitharam et al. (2008) have evaluated the undrained response from drained triaxial test result considering spherical particles and the results have been qualitatively compared those with experimental results. Studies by Ng and Dobry (1994) have clearly indicated that the use of particles having perfect round shape and uniform gradation results in excessive rotation and fails at lower shear strains compared to actual sands. The significance of particle shape on the engineering properties have been highlighted by Mirghasemi et al. (2002), Ashmawy et al. (2003), Cho et al. (2006), Pena et al. (2007).

It has been shown that spherical particles have a smaller angle of repose and reduced shear strength as compared to non-spherical particles (Rothenburg and Bathurst 1992). This can be attributed to the fact that for non-spherical particles the rotation can be inhibited by mechanical interlocking. 2-D shear studies done by Matsushima and Chang (2011) on irregularly shaped particles showed that the contribution of rotation and sliding mechanism can be related to the particle shape. Lu and McDowell (2007) have reported that it is possible to model a real granular material under static and cyclic conditions. Particle Flow Code (PFC ^{3D}) is used in this numerical study for the simulations of the triaxial testing of non-spherical particle assembly.

1 Research Scholar, Department of Civil Engineering, Indian Institute of Science, Bangalore - 560012, Email: anitha@civil.iisc.ernet.in

2 Professor, Department of Civil Engineering, Indian Institute of Science, Bangalore - 560012, Email: sitharam@civil.iisc.ernet.in

Numerical Simulations of Cyclic Undrained Tests

Simulations are conducted on a cylindrical assembly whose height to diameter ratio is 2:1 similar to that of a triaxial sample. Table 1 summarizes the properties of the sample used for the simulation.

Table 1 Properties Used For The Particles

Properties	Values
Normal contact stiffness of particle (K_n)	1e5N/m
Shear contact stiffness of particle(K_s)	1e5N/m
Wall stiffness (k)	1e6N/m
Particle density (ρ)	2650kg/m^3
Interparticle friction (μ)	0.5
Friction between particle and wall(μ)	0.3
Damping coefficient	0.7
Particle size used in the simulation (m)	0.001 - 0.004
Acceleration due to gravity	-9.81m/s^2

Figure 1 shows the cylindrical assembly used for the test. The simulations follow axisymmetric triaxial loading conditions. A typical clump which forms the ellipsoidal shaped particle is shown in Figure 2. The aspect ratio of the clumps used in this assembly is 1.5.This shape was achieved by using the clump logic available in PFC^{3D}. Clump logic allows the particles to be joined together to give the required shape and they behave as a rigid body. The difference between a clump and a bonded particle is that, whatever may be the force acting on a clump the particles comprising the clump will not break apart. The linear force displacement law was used in this study as Ng and Dobry (1994) has reported that the simple linear normal force-displacement law produces comparable results.

In the following sections, a detailed note on the tests conducted on a mixture of spherical and ellipsoidal particles (represented as Sample A) and 100% spherical particles (represented as sample B) are presented. Sample A consists of 70% spheres and 30% ellipsoids. Clumps are added to the assembly by replacing particles each of which has the same volume as its replaced particle. Both samples A and B were prepared at an initial void ratio of 0.66 and subjected to an isotropic confining pressure of 100kPa. By controlling the scaling of particle and clump sizes, the required packing is obtained.

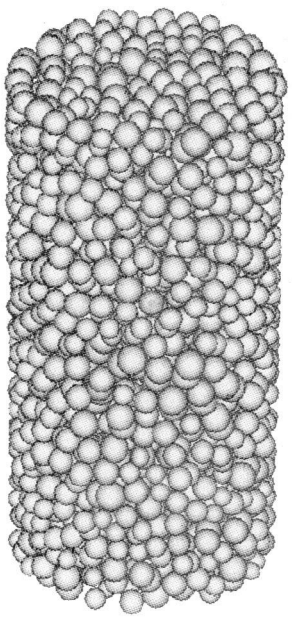

Fig. 1 Cylindrical Assembly

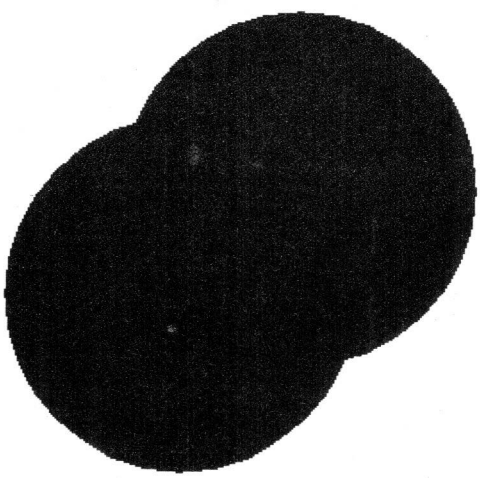

Fig. 2 Clump representing ellipsoid of aspect ratio of 1.5

Test procedure

Two sets of cylindrical assemblies were modeled for the tests. One set of cylindrical assembly consists of only spherical particles and the other set consists of a mixture of spherical and ellipsoidal particles. The assembly of particles formed is confined within top and bottom platens and a lateral cylindrical wall. The top and bottom platens are used to apply the loading whereas the lateral wall replicates the confinement experienced by the sample in triaxial testing. During the isotropic consolidation stage, the top and bottom wall velocities along with the radial velocity of the cylindrical wall are adjusted such that the sample is subjected to the required confining pressure. After the initial isotropic consolidation, a sinusoidal wave form was used for cyclic loading.

Constant strain amplitude cyclic undrained tests

Dobry et al. (1982) have pointed out that cyclic strain approach is more suitable to characterize liquefaction resistance. Hence cyclic strain approach is followed in this study. The undrained conditions are simulated by constant volume approach without explicitly incorporating the pore pressure. The generation of the excess pore pressure leads to a reduction in the effective stress resulting in the failure of the assembly. The excess pore pressure is calculated by taking the difference between the total stress path and effective stress path (Dobry and Ng, 1992). Cyclic loading under constant strain amplitude was done on isotropically consolidated samples at a confining pressure of 100kPa. The magnitude of the cyclic strain amplitude was set as 0.6%. These strains were applied sinusoidally at a frequency of 1Hz and continued until the deviatoric strength was almost reduced to zero.

Results and discussions of tests on spherical particles

The results of the cyclic undrained tests at a strain amplitude of 0.6%, void ratio 0.66 and frequency 1Hz are presented in the following figures. Figure 3(a) shows the variation of deviatoric stress q with mean stress p for a confining pressure of 100kPa. The plot clearly indicates the reduction in the mean stress and deviatoric stress as the loading progresses. The reduction in effective stress is attributed to the development of excess pore water pressure. The variation of deviatoric stress with axial strain is plotted in Figure 3(b). The degradation of the modulus can be clearly seen in this plot. The pattern of the results obtained is matching well with the already established laboratory results of several researchers for loose granular media.

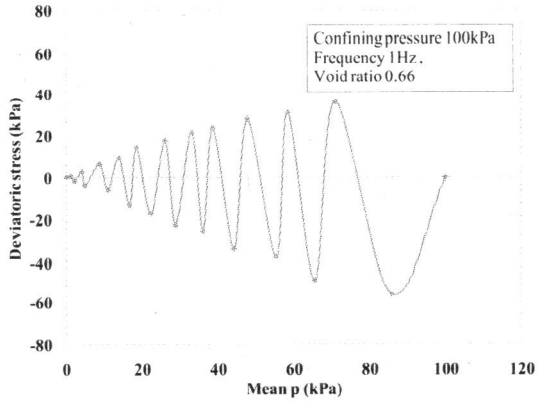

(a) Deviatoric stress q vs. mean p (Stress path)

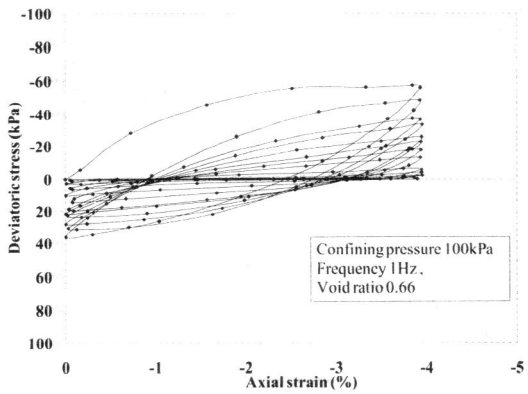

(b) Deviatoric stress vs axial strain

Fig. 3 Variation of parameters of the test assembly consisting of 100% spheres

Micromechanical interpretation

Whenever there is a change in shear stress in an assembly, force and fabric anisotropy steps in. The force anisotropy is quick to adjust itself with the applied stress changes but the fabric anisotropy takes some time to attain a compatible configuration. The internal parameters which control the micromechanics of the assembly include the average coordination number, contact force and contact normal. Figure 4 indicates the reduction in the average coordination number with mean stress and deviatoric stress. Basically the reduction in the mean stress as the excess pore water pressure increase is due to the loss of contacts as the loading progresses. When the average coordination number is around 3, the system becomes unstable and liquefaction occurs. This plot also indicates that along with the decrease in the average coordination number, the deviatoric stress also reduces and finally the assembly collapses. In order to interpret the behaviour from grain scale, the contact force distribution, contact normal distribution and displacement vectors are extracted and shown.

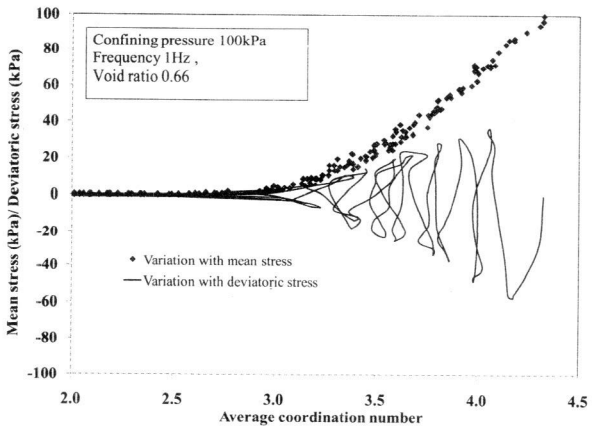

Fig. 4 Variation of average coordination number for 100% spheres

Figure 5(a) indicates the various micromechanical parameters of the assembly under isotropically consolidated conditions. The thickness of the lines indicates the magnitude of contact force. Also it can be seen that the force distribution is isotropic. Figure 5 (b) shows the distribution of contact force, displacement vector and contact normal at liquefaction. These redistributions are attributed to the fact that whenever there are stress changes in the assembly, an adjustment in the microstructure follows. This results in the introduction of force anisotropy in the system mainly through the drop of contacts in the minor stress direction. The loss of contacts is reflected as a decrease in the average coordination number which leads to a reduction in the effective mean stress. The break in the contact force chain due to the reduction in the average coordination number is ultimately responsible for the phenomena of liquefaction. Also the thickness of the contact force diagram reduces drastically indicating there is reduction in the contact force and density of contact normals. These results obtained for the spherical shaped particles matches qualitatively with the established experimental results of the cyclic behaviour of granular mass. A close examination of the contact force diagram at liquefaction reveals that the sample started liquefying from the centre towards the boundary. This can be attributed to the localization of deformation into thin zones of intense shearing at the centre part of the assembly. As suggested by Desrues and Viggiani (2004), the strain localization can initiate in the inner part of the specimen depending on the specimen geometry and propagate towards the rigid boundaries. The displacement vector diagram (Figure 5) indicates the displacement of each ball with the vector length proportional to the magnitude and orientation in the direction of the arrow. It is clear from this figure that the magnitude of the displacement has increased at liquefaction, but no significant changes have been observed in the orientation of the vector.

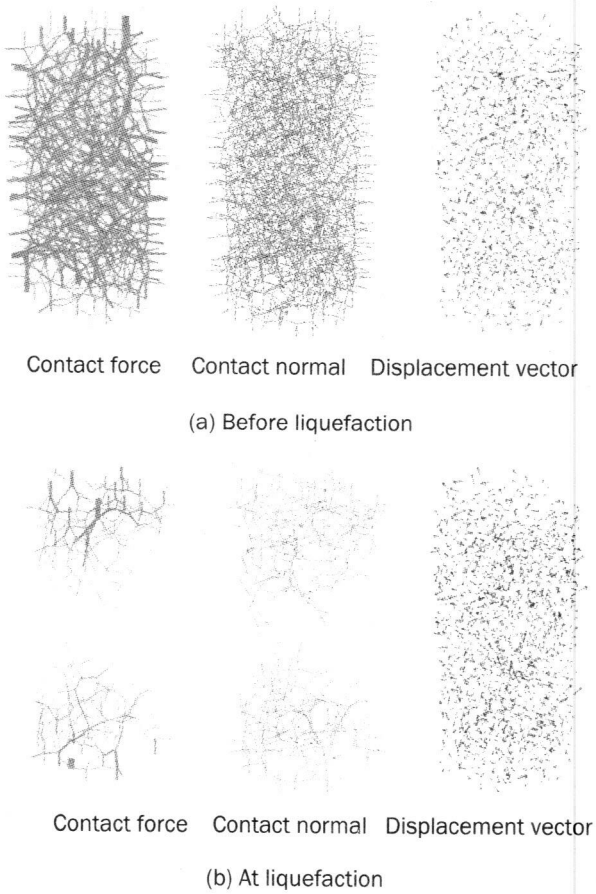

Fig. 5 Variation of microparameters before and after liquefaction for sample B

Results and discussions of tests on a mixture of spherical and elliptical particles

The cylindrical assembly consisted of a total of 1950 particles of which 585 particles (30% of the particles) are ellipsoids and the remaining are spheres. The ellipsoidal particles used in this simulation are having an aspect ratio of 1.5. The results of the cyclic undrained tests at a strain amplitude of 0.6%, void ratio 0.66, confining pressure 100kPa and frequency 1Hz are presented in Figure 6. Figure 6a (i) depicts the variation of deviatoric stress as the number of loading cycle progresses. This plot clearly signifies that the deviatoric stress reaches a maximum value in the first cycle and thereafter it progressively decreases. The variation of deviatoric stress with axial strain is plotted in Figure 6a (ii). The degradation of the modulus can be clearly seen in this plot. The reduction in effective stress is attributed to the development of excess pore water pressure as shown in Figure 6a (iii).

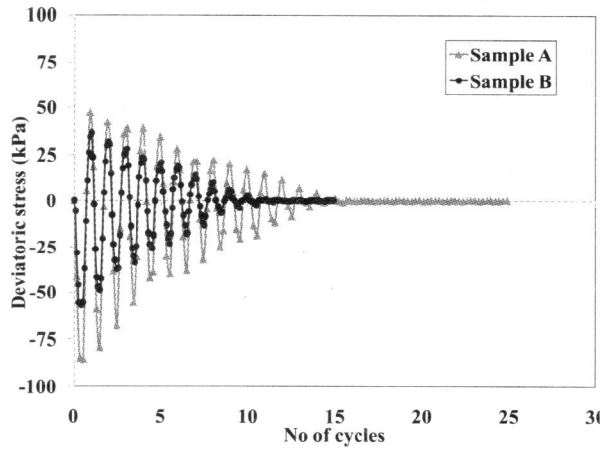

(i) Deviatoric stress vs. no of cycles

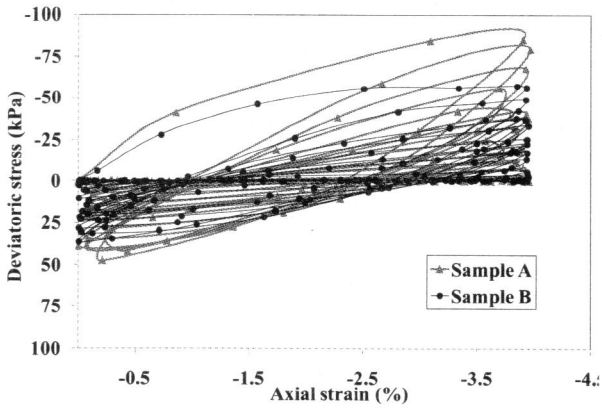

(ii) Deviatoric stress vs. axial strain

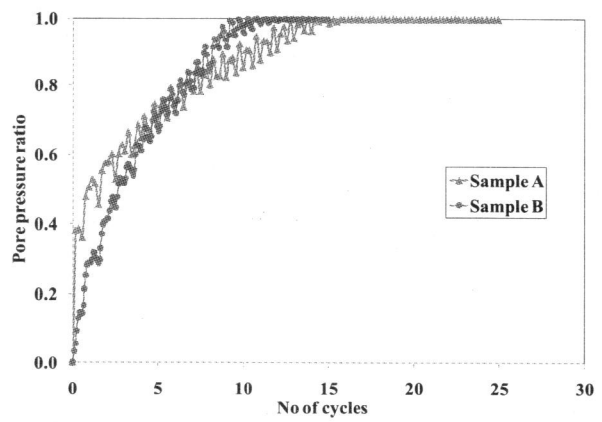

(iii) Pore pressure ratio vs. number of cycles

Fig. 6 (a) Comparison of various parameters for sample A and sample B

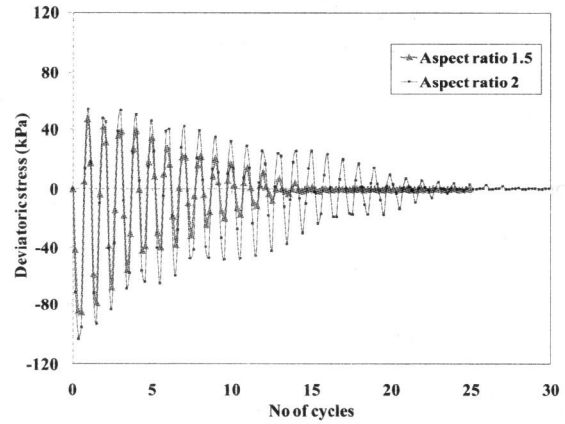

(iv) Deviatoric stress vs. no of cycles

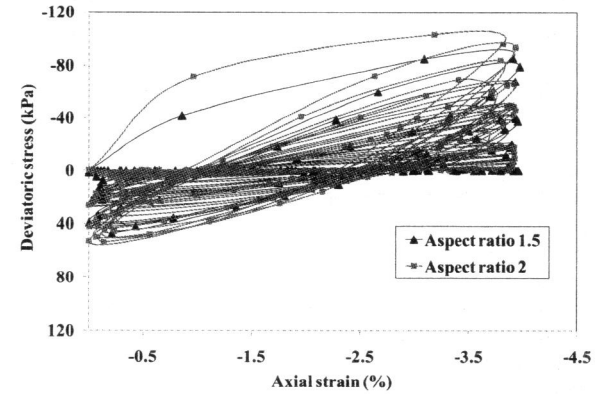

(v) Deviatoric stress vs. axial strain

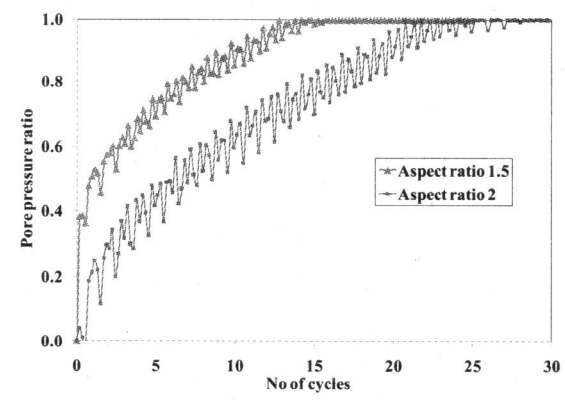

(vi) Pore pressure ratio vs. number of cycles

Fig. 6 (b) Comparison of various parameters for Sample A and Sample C

This increase in excess pore pressure forces the stress path to migrate towards the origin. From these three plots, it is seen that as the shape changes from sphere, there is an increase in the resistance to liquefaction. This increase can be attributed to the geometrical effects of non-spherical particles. An aspect ratio of 1.5 results in a larger plane surface allowing more number of contacts per particle. In addition to this the rolling motion of these particles are also restricted to a greater extent due to the strong interlocking among them. It is interesting to note that during the initial stages of loading, the rate of excess pore pressure generation is high for ellipsoidal particles whereas as the number of loading cycle increases, the rate of generation of excess pore pressure becomes faster for spheres. This can be attributed to the restrictions in the particle mobility due to irregularity thereby preventing the particles to attain a dense packing configuration. Also at small strains the deformations usually tend to localize at interparticle contacts (Cho et al, 2006). As the loading progresses, the particle rotation of the ellipsoidal particles is inhibited resulting in dilation and hence greater shear resistance.

To underline the shape aspect, comparative results of the stress path, stress strain and pore pressure ratio variation of two assemblies consisting of particles of different aspect ratios subjected to a confining pressure of 100kPa are presented in figures 6b(iv) - 6b(vi). First assembly consists of 30% clumps having aspect ratio 1.5 (Sample A) where as the second assembly consists of 30% clumps having aspect ratio 2.0 (represented as Sample C). These plots indicate that as aspect ratio increases, the number of load cycles required for the sample to liquefy increases at a confining pressure of 100kPa. Also the rate of development of pore pressure is also affected by this factor.

Micromechanical Interpretation

The internal parameters which control the micromechanics of the assembly include the average coordination number, contact force and contact normal. Figure 7 indicates the reduction in the average coordination number with mean stress and deviatoric stress. It can be seen that the sample containing ellipsoidal particles is having an initial coordination number of 6 whereas for spherical assembly it is just above 4. This change in coordination number is due to the fact that the irregular shape results in a much larger contact plane and subsequently more number of contacts per particle. As evident from this plot, after an initial sudden drop in the average coordination number for the sample consisting of ellipsoidal particles, the reduction is almost linear. At the same time, for the assembly consisting of only spheres the drop is gradual. This sudden drop in sample A compared to sample B is reflected in the plot (Figure 6a (iii)) as a sharp increase in the rate of excess pore pressure generation. When the average coordination number is around 3 for spheres and 4 for the assembly consisting of spheres and ellipsoids, the system becomes unstable and liquefaction occurs. The variation of average coordination number with deviatoric stress also indicates the same trend.

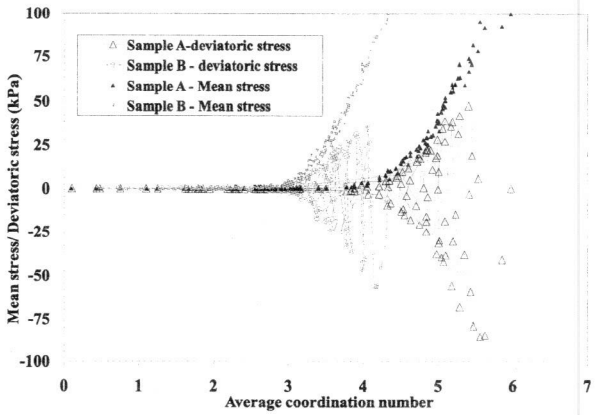

Fig. 7 Variation of average coordination number for sample A and sample B

Figure 8 indicates the micromechanical parameters like contact force and displacement vectors of the assembly under isotropically consolidated conditions and at liquefaction for all the three types of assemblies. The thickness of the lines indicates the magnitude of contact force. Also it can be seen that the force distribution is isotropic initially. The redistribution of contact force at liquefaction is attributed to the fact that whenever there are stress changes in the assembly, an adjustment in the microstructure follows. This results in the introduction of force anisotropy in the system mainly through the drop of contacts in the minor stress direction. The loss of contacts is reflected as a decrease in the average coordination number which leads to a reduction in the effective mean stress or an increase in pore pressure ratio. It is interesting to note that there are almost nil contacts at certain parts of the assembly and is evident from the average coordination number less than 1. Similar to the results obtained for the spherical particles alone, the break in the contact force chain due to the reduction in the average coordination number resulted in the phenomena of liquefaction. The reduction in the thickness of the contact force diagram also indicates a decrease in the contact force and density of contact normal. A close examination of the contact force and contact normal at the start of the shearing stage indicates a dense distribution for the assembly consisting of ellipsoids than the assembly of 100% spheres. This dense packing of the assembly results in a higher coordination number and subsequent higher resistance to liquefaction as evident from the various plots already shown in Figures 6. Moreover it is observed that the sample started liquefying from the

centre and slowly progresses towards the boundary. Pena et al (2007) have pointed out from two dimensional discrete element simulations that the orientation of the contacts in the steady state in the case of non-spherical particles is governed by the particle orientation. Basically the particles will try to orient themselves such that the packing is stable. The variation of contact forces as shown in Figure 8 (c) indicates the make and break of the force chain as the loading progresses. These results show that during the initial loading cycles force chain weakens considerably along the vertical direction which in turn suggests that the contact points lie on flat surfaces thereby trying to give a stable configuration to the whole assembly. Towards the final stages, the contacts are broken in both vertical and horizontal directions and ultimately leading to complete collapse.

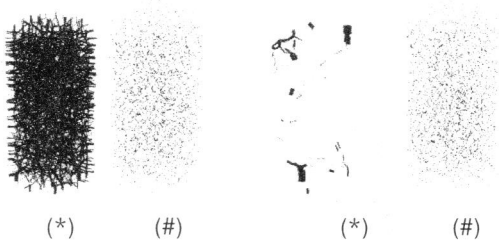

(a) Microparameters for sample A before and at liquefaction

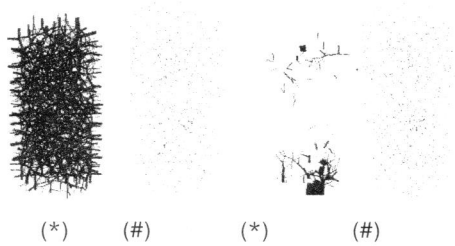

(b) Microparameters for sample B before and at liquefaction

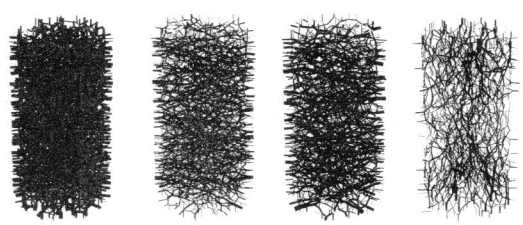

(c) Variation of contact force for sample C

(*)- Contact force , (#) – Displacement vector

Fig. 8 Variation of microparameters for sample A, sample B and sample C

Post Liquefaction Behaviour

The behaviour of sand after liquefaction is very important due to the fact that ground deformations follow earthquake loading. Usually loose granular soils undergo vertical and lateral displacements due to the densification of these soils subjected to rapid cyclic loading. A proper evaluation of the earthquake induced displacement helps to understand the resistance of the considered soil to monotonically increasing static loads. Sitharam et al. (2009) has reported that the post-liquefaction undrained static behaviour depends on the fabric of the assembly during liquefaction. In this section, a comparative study of the effect of particle shape on the post liquefaction behaviour of granular material subjected to undrained shear loading is presented.

Numerical Simulations of Undrained Post Liquefaction Behaviour

Assemblies made of spheres alone and a mix of spheres and clumps are used for this simulation. The state of the sample which is already liquefied was saved and the same is used for this analysis. The samples prepared and loaded which subsequently liquefied as explained in the previous section is used for simulating the undrained post liquefaction behaviour. The liquefied samples from both sets are subjected to undrained shear loading by applying an axial strain rate of 0.6%. Figure 9(a) shows the shear stress axial strain variation of both the assemblies. It can be seen that for small strains, the shear stress is almost zero. The variation of average coordination number with axial strain is shown in Figure 9(b). The variation of pore pressure ratio with axial strain is plotted in Figure 9(c). The slope of the curve indicates that the sample consisting of particles with aspect ratio 1.5, rearranges in a faster rate thereby developing more contacts and hence a rapid increase in the mean effective stress. Also, at an axial strain of 10% it is observed that the pore pressure ratio has become positive indicating dense specimen behaviour.

Micromechanical Interpretation of Post Liquefaction Behaviour

The infinitely small stiffness for very small strains can be attributed to the complete collapsed structure of the assembly. As loading progresses, shear stresses gradually increase and Figures 10(a) and 10(b) show that at around 10% axial strain there is significant increase in the contact force and contacts distribution.

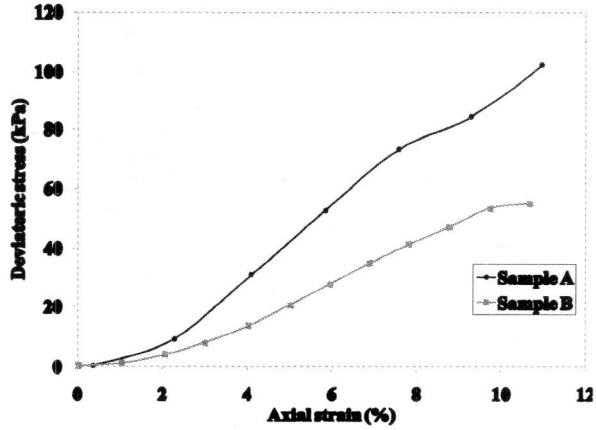

(a) Deviatoric stress vs axial strain

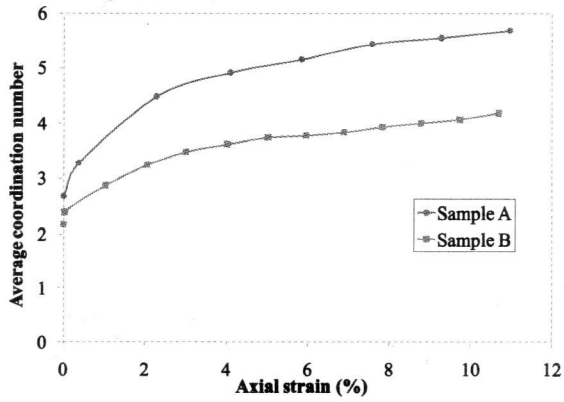

(b) Average coordination number vs axial strain

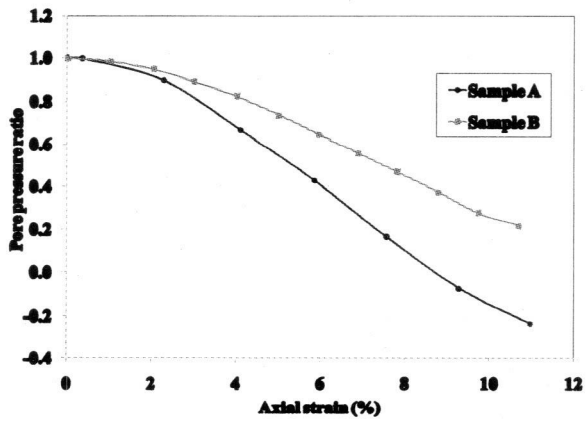

(c) Pore pressure vs axial strain

Fig. 9 Variation of parameters in post liquefaction undrained loading conditions for sample A and sample B

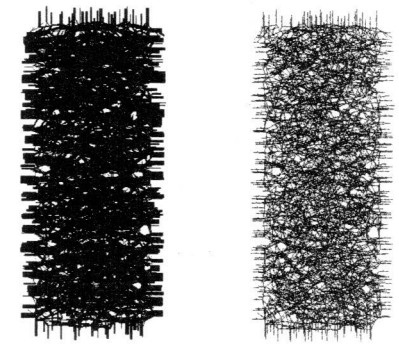

Contact force Contacts distribution

(a) for sample A

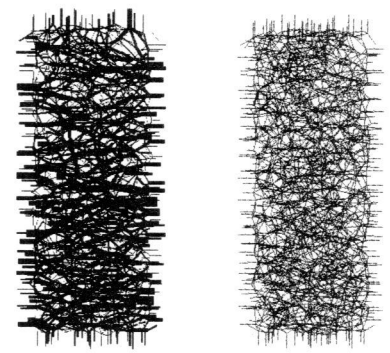

Contact force Contacts distribution

(b) for sample B

Fig. 10 Microparameters at 10% axial strain for samples A and B

This results in a more stable configuration of the particles which can be attributed to the increase in the stiffness of the assembly as evident from Figure 9(a). It is observed that the rate of increase of stress is much higher for the assembly consisting of clumps. This can be explained from the gain of contact forces and average coordination number. Figure 10(a) shows the contact force and contacts distribution of the assembly consisting of 30% ellipsoids. A comparison with Figure 10(b) clearly shows the denseness of the contact force and contact distribution for this assembly which can also be seen from figure 9(b) in terms of average coordination number. A critical examination of the development of contact force (Figure 10) confirms that more contacts are formed in the horizontal/minor principal stress direction and hence the horizontal contact forces have increased significantly. As the excess pore pressure reduces, the settlement occurs stage by stage leading to the formation of a layered structure. Scott (1986) has reported that following liquefaction the soil grains settle out and the material

solidifies from base up. This suggests that the accumulating sand layer is consolidating as time passes and thus forms a layered structure and is well evident from the contact force distribution diagram. During this settling it is possible that the particles will occupy a position which provides a stable configuration for the entire assembly. All these results strongly underline the influence of particle shape in the liquefaction and post-liquefaction behaviour of granular matter.

Conclusions

This paper has attempted to understand the effect of particle shape during the liquefaction and post liquefaction behaviour of granular material. The results indicate that particle shape is having a strong influence on the behaviour of these materials when prepared at the same void ratio. The increase in the initial coordination number due to the geometrical effects of non-spherical particles leads to the subsequent increased shear resistance of the assembly. Also the dilation resulting from the restrictions in particle rotation of the ellipsoidal particles add to the increased resistance to liquefaction. The variation of contact force distribution indicates that the contact points lie on flat surfaces as the particles try to orient themselves to give a stable configuration to the whole assembly. The observations also indicate that the sample started liquefying from the centre and slowly progressing towards the boundary. The various vectors indicate that the strain localization initiate in the inner part of the specimen and propagate towards the rigid boundaries. An analysis of the micro-parameters associated with post liquefaction behavior shows that the stiffness and strength are considerably higher for an assembly consisting of particles other than spheres. The post-liquefaction studies reveal that the assembly consisting of a mix of spheres and ellipsoids develops shear stress at a much faster rate which can be attributed to the rate of gain of contacts and contact forces owing to more contacts per particle. Another significant observation is the formation of more contacts in the horizontal/minor principal stress direction. The results obtained here further substantiate the need to address and understand the importance of particle shape in the dynamic properties of the granular matter.

References

Ashmawy, A. K., Sukumaran,B. and Vinh Hoang, V. (2003): 'Evaluating the influence of particle shape on liquefaction behaviour using discrete element modeling', *Proc.13th International Offshore and Polar Engineering Conference., ISOPE*, Honolulu, No. 2, pp. 542-549.

Cundall, P.A. and Strack, O.D.L. (1979): 'A Discrete Numerical Model for Granular Assemblies', *Geotechnique* 29(1), pp. 47-65.

Desrues, J. and Viggiani, G. (2004): 'Strain localization in sand: an overview of the experimental results obtained in Grenoble using stereophotogrammetry', *International journal for numerical and analytical methods in geomechanics* 28, pp. 279-321.

Dobry, R., Ladd,R.S., Chang,R.M. and Powell,D. (1982): 'Prediction of pore water pressure build up and liquefaction of sands during earthquakes by the cyclic strain method', *NBS Building Science Series* 138, Washington, DC, pp. 1-50.

Dobry, R. and Ng, T.T. (1992): 'Discrete modeling of stress-strain behaviour of granular media at small and large strains', *Engineering Computations*,9, pp.129-143.

Gye-Chun Cho., Dodds, J. and Santamarina, J. C. (2006): 'Particle shape effects on Packing Density, Stiffness and Strength: Natural and Crushed Sands', *Journal of geotechnical and geoenvironmental engineering*, 132(5), pp. 591-602.

Ishihara, K., Tatsuoka, F. and Yasuda, S. (1975): 'Undrained deformation and liquefaction of sand under cyclic stresses', *Soils and Foundations*, 15(1), pp. 29-44.

Itasca Consulting Group (2004): Particle Flow Code in Three Dimensions (PFC^{3D}) Manual.

Lu, M., McDowell, G.R. (2007): 'The importance of modelling ballast particle shape in the discrete element method', *Granular Matter* 9, pp. 69–80.

Mirghasemi,A.A., Rothenburg, L. and Matyas, L. (2002): 'Influence of particle shape on engineering properties of assemblies of two-dimensional polygon-shaped particles', *Geotechnique*, 52(3), pp. 209-217.

Ng, T. T. and Dobry, R. (1994): 'Numerical simulations of monotonic and cyclic loading of granular soil', *Journal of Geotechnical Engineering*, 120(2), pp. 388-403.

Norris G., Siddharthan R., Zafir Z. and Madhu, R. (1997): 'Liquefaction and Residual Strength of Sands from Drained Triaxial tests', *Journal of Geotechnical and Geoenvironmental Engineering*, 123(3), pp. 220-228.

Pena, A. A., Garcia-Rojo, R. and Herrmann, H. J. (2007): 'Influence of Particle shape on sheared dense granular media', *Granular Matter*, 9, pp. 279-291.

Rothenburg L. and Bathurst R. J. (1992): 'Micromechanical features of granular materials with planar elliptical particles', *Geotechnique*, 42 (1), pp. 79–95.

Scott, R.F. (1986): 'Solidification and Consolidation of a Liquefied Sand Column', *Soils and Foundations*, 26(4), pp. 23-31.

Seed, H. B. and Lee, K. L.(1966): 'Liquefaction of Saturated Sands During Cyclic Loading', *Journal of Soil Mechanics and Foundation Division*, 92(SM6), pp.105-134.

Sitharam, T.G., Dinesh, S. V. and Shimizu, N. (2002): 'Micromechanical modelling of monotonic drained and undrained shear behaviour of granular media using three dimensional DEM', *International Journal for Numerical and Analytical Methods in Geomechanics*, 26, pp. 1167-1189.

Sitharam, T. G. (2003): 'Discrete element modeling of cyclic behaviour of granular materials', *Geotechnical and Geological Engineering*, 21(4), pp. 297 - 329.

Sitharam, T.G., Vinod, J.S. and Ravishankar, B.V. (2008): 'Evaluation of undrained response from drained triaxial shear tests: DEM simulations and experiments', *Geotechnique* 58(7), pp. 605-608.

Sitharam, T. G. and Vinod, J. S. (2008): 'Numerical simulation of liquefaction and pore pressure generation in granular materials using DEM', *International Journal of Geotechnical Engineering*, 2 (2), pp. 103-113.

Sitharam, T.G., Vinod, J.S. and Ravishankar, B.V. (2009): 'Post liquefaction undrained monotonic behaviour of sands: experiments and DEM simulations', *Geotechnique* 59(9), pp. 739-749.

Takashi Matsushima. and Ching.S.Chang. (2011): 'Quantitative evaluation of the effect of irregularly shaped particles in sheared granular assembiles', *Granular matter,* 13, pp. 269-276.